Received: 22 July 2018 | Revised: 2 November 2018 | Accepted: 7 November 2018

DOI: 10.1002/er.4313

RESEARCH ARTICLE

WILEY INTERNATIONAL JOURNAL OF ENERGY RESEARCH

Modeling representative Gen-IV molten fuel reactivity effects in the ZEPHYR ZPR - LFR analysis

Marat Margulis[1,2] | Patrick Blaise[2] | Erez Gilad[1]

[1] The Unit of Nuclear Engineering, Ben-Gurion University of the Negev, Beer-Sheva, Israel

[2] DEN/CAD/DER/SPESI, CEA Cadarashe, CEA Cadarache, Saint-Paul-les-Durance, France

Correspondence
Erez Gilad, The Unit of Nuclear Engineering, Ben-Gurion University of the Negev, Beer-Sheva 84105, Israel.
Email: gilade@bgu.ac.il

Funding information
Israeli Ministry of Energy, Grant/Award Number: 215-11-020

Summary

Studies related to severe core accidents constitute a crucial element in the safety design of Gen-IV systems. A new experimental program, related to severe core accidents studies, is proposed for the zero-power experimental physics reactor (ZEPHYR) future reactor. The innovative program aims at studying reactivity effects at high temperature during degradation of Gen-IV cores by using critical facilities and surrogate models. The current study introduces the European lead-cooled system (ELSY) as an additional Gen-IV system into the representativity arsenal of the ZEPHYR, in addition to the sodium-cooled fast reactors. Furthermore, this study constitutes yet another step towards the ultimate goal of studying severe core accidents on a full core scale. The representation of the various systems is enabled by optimizing the content of plutonium oxide in the ZEPHYR fuel assembly. The study focuses on representing reactivity variation from 900°C at nominal state to 3000°C at a degraded state in both ELSY and Advanced Sodium Technological Reactor for Industrial Demonstration (ASTRID) cores. The study utilizes the previously developed calculation scheme, which is based on the coupling of stochastic optimization process and Serpent 2 code for sensitivity analysis. Two covariance data are used: the ENDF 175 groups for ELSY and the Covariance Matrix Cadarache (COMAC) 33 groups for ASTRID. The effect of the energy group structure of the covariance data on the representativity process is found to be significant. The results for single degraded ELSY fuel assembly demonstrate high representativity factor (>0.95) for reactivity variation and for the criticality level. Also, it is shown that the finer energy group structure of the covariance matrices results in dramatic improvement in the representation level of reactivity variations.

Glossary: S_E, Experimental system sensitivity vector; S_R, Reference system sensitivity vector; V, Variance-covariance matrix; ϵ_E, Experimental system propagated uncertainty; ϵ_R, Reference system propagated uncertainty; r_{RE}, Representativity factor; ϵ_R^*, Reactor response uncertainty; ω, Experimental weight or experimental importance; δE, Experimental uncertainty; R_0, Priori calculated values; $\widehat{R}$, Posteriori calculated values; α, Transposition factor
Acronyms: ALFRED, Advanced Lead-Cooled Fast Reactor European Demonstrator; ASTRID, Advanced Sodium Technological Reactor for Industrial Demonstration; CEA, Commissariat à l'Énergie atomique et aux Énergies Alternatives; CFV, Reduced void fraction; COMAC, Covariance Matrix Cadarache; ELSY, European lead-cooled system; Gen-IV, Generation IV; LFR, Lead-cooled fast reactor; LWR, Light water reactor; MYRRHA, Multipurpose Hybrid Research Reactor for High-Tech Applications; ND, Nuclear data; NK, Neutronic kinetics; SCA, Severe core accident; SFR, Sodium-cooled fast reactor; TH, Thermal hydraulics; UCOM, Updated covariance matrix; ZEPHYR, Zero-power experimental physics reactor; ZPR, Zero-power reactor

KEYWORDS

ASTRID, core meltdown, ELSY, nuclear power, nuclear reactor safety, representativity, severe accident, ZEPHYR

1 | INTRODUCTION

Safety of nuclear reactors is essential for the future prospects of nuclear energy as a reliable, affordable, and clean source of energy. Safety standards are continuously reviewed and upgraded as new research and development are performed. Continuous research, improved standards, and new evaluable experiments regarding this subject are of fundamental importance for the nuclear industry. Since the Fukushima Daichii accident, there have been many analyses of its causes, consequences, and implications leading to countless new measures taken worldwide by the nuclear community.[1,2] These measures include the reassessment of current and future designs of nuclear power plants (as well as research reactors and critical facilities) against extreme accidental conditions.

A key aspect in the design of nuclear power system is the prevention, monitoring, and mitigation of postulated severe core accidents (SCA). The accidents at TMI-2 and Chernobyl raised the awareness for this kind of accidents and emphasized the importance of SCA studies. Nonetheless, there still exist many unknown factors in our understanding of SCA progression, as was demonstrated by the Fukushima Daichii accident in 2011.[3,4] Adequate analyses are needed for all phases of severe accident's progression in order to improve the safety margins of the design. The main gaps related to pressurized water reactors (PWRs) that require further research are identified by the EUROSAFE forum.[3] These include problems related mainly to mechanical, chemical, and material problems, which are all related to the reactor's behavior during an SCA.

The analysis of hypothetical core disruptive accidents in liquid metal fast reactors is a central point in their safety assessment since their development.[4,5] When considering SCA in Gen-IV future systems,[6] such as sodium-cooled fast reactors (SFRs) and lead-cooled fast reactors (LFRs), the SCA progression is strongly coupled to the neutronic behavior of the core. This feature, which constitutes a major difference from light water reactors (LWRs), results from the fact that fast core configurations (ie, material balance and geometry) do not create the most reactive configuration. Therefore, changes to the core layout, ie, material relocation in the core due to SCA (eg, fuel, coolant, structural materials), can potentially lead to positive reactivity insertion and uncontrolled power excursion. Therefore, a detailed study of SCA progression is required to estimate the neutronic characteristics of the core during different stages of SCA.[7]

It is impractical to perform neutronic experiments related to SCA because it would have to involve a critical core undergoing meltdown at 3000°C. This melted core might experience large positive reactivity ramp. Large positive reactivity ramps may be introduced in the system because of compaction of melt fuel in core regions characterized by a significant neutronic contribution triggered by, eg, sloshing phenomena during the transition phase.[8] Hence, most of the R&D related to neutronic behavior during SCA is based on computer simulations. Since SCA in Gen-IV reactors is a strongly coupled neutronic, thermal-hydraulic, and thermomechanic process, multiphysics codes, also known as "best-estimate" codes (eg, high-fidelity coupled NK/TH codes), are usually utilized. For that reason, a neutronic-related experimental program for studying SCA progression is of utmost importance for the continued qualification of computational tools (eg, best-estimate codes) and monitoring instrumentation.

The progression of SCA in a nuclear reactor is a nonlinear stepwise process, which can develop in a wide range of directions with a large number of associated degraded configurations. Moreover, the SCA progression timescale is extremely slow with respect to the neutronic timescale. Hence, the study of neutronic behavior during SCA can be performed utilizing a quasistatic approach for studying instantaneous configurations, which are realized in the course of the meltdown process. This is obtained by validating computational results versus *relevant* experimental data gathered in a critical facility. The importance of "representative" experimental programs emerges from this crucial need to transfer (or "translate") experimental data, measured in a zero-power reactor, to the equivalent information in the reference power system. Hence, "best-representative" experiments are crucial for the design stage of safety features for nuclear power systems (current and future).

High representativity of numerous integral parameters, eg, criticality or reactivity variations, enables to provide a best-estimate neutronic analysis of the system being investigated in a safe and flexible setting of a zero-power reactor (ZPR).[9,10] Essentially, representative experiments provide information on physical (neutronic) quantities of the investigated power system, eg, criticality, reactivity changes, flux distribution, spectrum, reactivity feedbacks, by appropriate experimental measurements and analysis in a mock-up system.

Previous studies showed that highly representative SCA configurations (ie, with high representativity factor) can be obtained on a single SFR fuel assembly level.[7]

The previous work[7] focused on the Advanced Sodium Technological Reactor for Industrial Demonstration (ASTRID) reduced void fraction (CFV) core.[11] Recent developments related to the ASTRID project experienced substantial modifications,[12] with a significant reduction in power (from 600 MWe to 100-200 MWe). Nevertheless, the ASTRID CFV concept presents an interesting challenge in terms of severe accident studies, due to the high heterogeneity of the core. In light of these recent developments, the Commissariat à l'Énergie Atomique et aux Énergies Alternatives (CEA) decided to expand the scope of its severe accidents studies beyond ASTRID-like SFR designs. This step is supposed to assist in ensuring the high scientific and industrial attractiveness of the planned experimental reactor zero-power experimental physics reactor (ZEPHYR).[13] This paper describes the extension of the ZEPHYR representativity capabilities beyond the ASTRID-like core to include the European lead-cooled system (ELSY)[14] on the level of a fuel assembly.

The extension of the representativity capabilities of the ZEPHYR reactor is facilitated, to a large extent, by the unique nuclear fuel stockpile of the MASURCA reactor, available at CEA research center at Cadarache. This stockpile contains a wide variety of fuel materials (MOX, enriched UO_2, metallic uranium, and plutonium,) in different geometries (pins, plates, bars, slabs) and representative coolant channels (sodium and lead). The availability of this fuel stockpile provides a high degree of flexibility in the design of an experimental ZEPHYR core. This is a significant advantage to the proposed experimental program thanks to the possibility that high representative core configuration can be designed and built using the existing fuel stockpile without the need for additional new fuel manufacturing.

This paper focuses on representativity studies on the level of a single fuel assembly of the ELSY configuration and its representation during SCA conditions. This study constitutes an essential and initial step towards further qualification of the methodology on a full core scale SCA for both the SFR and LFR cores in the ZEPHYR facility.

Nuclear data will be addressed by ZEPHYR through integral measurements in various spectra, thanks to the flexibility in the built configurations: from thermal to fast. Nuclear data represent now the major source of uncertainty on integral parameters. Any improvement in ND will enhance all core physics parameters and, by extension, any criticality and safety issues.

In Section 2, the methodology developed for designing best-representative experiments is detailed, and a short overview of the ZEPHYR project is presented, as well as a description of the two Gen-IV reference systems (ASTRID and ELSY) considered in this study. In Section 3, the results of best-representative experiment design for a single ELSY LFR fuel assembly are described and discussed, and the representativity of a single ASTRID SFR fuel assembly is revisited. Conclusions and discussion are presented in Section 4.

2 | METHODOLOGY AND EXAMINED SYSTEMS

In this section, the methodology developed and implemented for designing best-representative core configurations is described. In addition, the mathematical model of the representativity process is summarized, and the Gen-IV nuclear systems under investigation are described, ie, ZEPHYR, ASTRID-CFV, and ELSY.

2.1 | Representativity method

The representativity model is based on a method proposed in the previous study.[15] The importance of best-representative experiment design stems from its capability to transfer (or "translate") experimental data, measured in a mock-up facility, to the equivalent information in the reference power system. This is of great potential for supporting the design of future systems, eg, the molten salt-cooled reactor experiments recently launched at Petten, Netherlands.[16] Nuclear data of salts are not experimentally studied, and some important lacks remain.[17] Technically, ZEPHYR can reproduce a representative MSR spectrum (even probably some mock-up if the fuel is solid). Through oscillation of a molten salt sample, it should be possible to target the proper ND and improve it.

The underlying hypothesis relies on a comparison between the sensitivity profiles of the quantity under investigation. The similarity is quantified using the representativity coefficient (r_{RE}), as defined in Equation 1,[15]

$$r_{RE} = \frac{\boldsymbol{S}_{\boldsymbol{R}}^{t} \boldsymbol{V} \boldsymbol{S}_{\boldsymbol{E}}}{\sqrt{\boldsymbol{S}_{\boldsymbol{R}}^{t} \boldsymbol{V} \boldsymbol{S}_{\boldsymbol{R}}} \sqrt{\boldsymbol{S}_{\boldsymbol{E}}^{t} \boldsymbol{V} \boldsymbol{S}_{\boldsymbol{E}}}} \equiv \frac{\boldsymbol{S}_{\boldsymbol{R}}^{t} \boldsymbol{V} \boldsymbol{S}_{\boldsymbol{E}}}{\epsilon_R \epsilon_E} \tag{1}$$

where $\boldsymbol{S}$ represents the response vector (sensitivity) of the integral quantity to nuclear data (ND) in the two different systems, the subscript $\boldsymbol{E}$ stands for the experimental representative mock-up, the subscript $\boldsymbol{R}$ stands for the reference systems, and $\boldsymbol{V}$ represent nuclear data covariance matrix.

In Equation 1, the numerator denotes the covariance between the experimental mock-up and the reference power system responses, while the terms in the denominator, ie, $\boldsymbol{S}_{\boldsymbol{R}}^{t} \boldsymbol{V} \boldsymbol{S}_{\boldsymbol{R}}$ and $\boldsymbol{S}_{\boldsymbol{E}}^{t} \boldsymbol{V} \boldsymbol{S}_{\boldsymbol{E}}$, denote the priori variance (uncertainty) of the relevant quantity in systems $\boldsymbol{E}$ and $\boldsymbol{R}$ due to uncertainties in the nuclear data, respectively, which are propagated using the sandwich rule.[18] The more the reference sensitivity ($\boldsymbol{S_R}$) is similar to the experimental sensitivity ($\boldsymbol{S_E}$), the closer the representativity factor (r_{RE}) is to unity. A representativity factor close to unity indicates that the two systems are highly correlated in terms of neutronic sensitivities (of the relevant quantity) with respect to the covariance data $\boldsymbol{V}$.

In the previous analysis,[7] the Covariance Matrix Cadarche V01 (COMAC-V01) and the JEFF-3.1.1 nuclear data evaluation were utilized in the representativity process. However, the COMAC-V01 does not contain information on lead. Therefore, the ENDF/B-VII.1[19] nuclear data evaluation was utilized together with the publicly available covariance matrix, which can be obtained from the Nuclear Energy Agency (NEA) Java-Based Nuclear Data Information System (JANIS).[20] The sensitivity vectors were calculated using the Serpent v2.1.29 Monte Carlo code.[21]

The application of the representativity method for the design of an experimental system enables the prediction of a posteriori reduction factor in the reactor response uncertainty (ϵ_R^*) once the experimental information is assimilated. The reduction factor is given by

$$\left(\epsilon_R^*\right)^2 = \left(\epsilon_R\right)^2\left(1-\omega r_{RE}^2\right), \tag{2}$$

where $\omega = \left(1+\delta E^2/\epsilon_{\boldsymbol{E}}^{\boldsymbol{2}}\right)^{-1}$ is called "experimental weight" factor, or an "experimental importance," and δE is the experimental uncertainty. This factor is a measure for the accuracy of the integral physical quantity in the representative system with respect to the nuclear data propagated uncertainty associated with it. In the case $r_{RE} = 1$ and $\delta E^2/\epsilon_{\boldsymbol{E}}^{\boldsymbol{2}} \to 0$, the reduction factor, ie, ϵ_R^*/ϵ_R, vanishes. However, this is not the case as shown in what follows. The C/E bias from the experimental parameter can be transpositioned to the target parameter bias $\widehat{R}-R_0$ (posteriori and priori calculated values) that can be written as follows:

$$\frac{\widehat{R}-R_0}{R_0} = \alpha\left(\frac{E-C}{C}\right) \tag{3}$$

where E is the experimentally measured parameter, C is the calculated parameter, and the transposition factor α is expressed as[22]

$$\alpha = \frac{\boldsymbol{S_R^t V S_E}}{\delta E^2 + \epsilon_{\boldsymbol{E}}^{\boldsymbol{2}}} = \omega r_{RE}\frac{\epsilon_R}{\epsilon_E} \tag{4}$$

2.2 | The ASTRID CFV-V0 core

The ASTRID concept was proposed following the sustainability requirements and safety standards that were determined in the roadmap for Gen-IV nuclear energy systems.[6] The selection of an SFR system for the ASTRID project was based, to a large extent, on the extensive and invaluable experience of the French nuclear industry with the PHENIX and SUPERPHENIX SFR systems. In recent years, several core layouts were proposed for the ASTRID core.[23] A most promising concept was found to be the reduced void fraction (CFV) core, arranged in a hexagonal lattice and consists of four axial regions: the lower blanket, the lower fissile zone, the intermediate blanket, and the upper fissile zone, as described in Figure 1. The main parameters of the CFV-V0 are given in Table 1.

2.3 | European lead-cooled system

Similar to the SFR, lead-cooled fast reactor (LFR) is also one of the six fast systems selected by the Gen-IV forum as best candidates to comply with the future requirements of the nuclear industry. LFRs present some advantages in terms of safety in unprotected severe accidents,

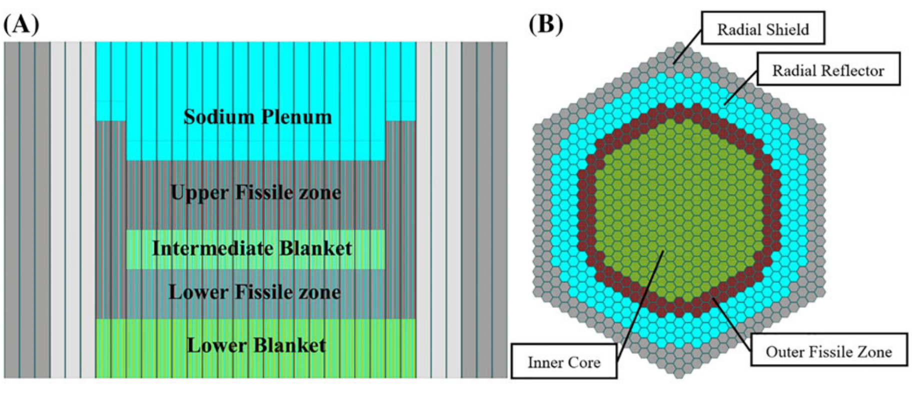

FIGURE 1 ASTRID CFV-V0 core layout: (A) axial cut and (B) radial cut [Colour figure can be viewed at wileyonlinelibrary.com]

TABLE 1 The CFV-V0 core design[11]

Parameter	
Power, MWth	1500
Primary coolant	Sodium
Inner core dimensions	
• Lower blanket height, cm	30
• Lower fissile zone height, cm	25
• Intermediate blanket height, cm	20
• Upper fissile zone height, cm	35
• Inner core radius, cm	133
• Assembly pitch, cm	17.5
Outer fissile zone dimensions	
• Lower blanket height, cm	30
• Fissile zone height, cm	100
• Outer fissile zone radius, cm	163
• Assembly pitch, cm	17.5
Plutonium oxide enrichment (inner/outer fissile zones), %	23/23
Effective delayed neutron fraction (β_{eff}), pcm	364
Reactivity worth of 100% void, $	−1.2

mainly thanks to the high boiling temperature of lead (about 1750°C) with respect to SFRs (sodium boiling temperature about 883°C). However, lead as a coolant is not free of faults. The main challenge in lead-cooled systems is the erosion of protective oxide layers, leading to enforcing an upper limit on coolant velocity (around 2.5-3 m/s).[24] This limitation practically reduces the heat removal capability of the lead with respect to sodium (typical sodium flow velocity is around 10 m/s). As a result, the pinwise pitch in LFR is larger than in SFR, resulting in better fluid circulation and enhanced safety performances. Corrosion of structural materials is also a major concern in future LFR systems. One possible way to overcome the corrosion problem is through controlling the oxygen content in the lead. Such technology was used in the Russian Alpha-class submarines, which was effective at temperatures up to 820°K.[25]

Considering the two systems, LFRs present safety-related advantages during unprotected severe accidents, mainly due to a better natural circulation and the higher boiling temperature. However, the corrosion of structural materials can lead to blockages of flowing channels, which can be followed by complete channel voiding. Moreover, the experience with LFR is very limited (mainly in the Russian Alpha-class submarines), and public information is unavailable. Therefore, these systems must go through further investigation before construction, making the ZEPHYR facility an excellent candidate to serve as an experimental mock-up.

Several LFR concepts are currently under investigation worldwide: the accelerator-driven system Multipurpose Hybrid Research Reactor for High-Tech Applications (MYRRHA) in SCK Belgium,[26] the BREST-300 and BREST-1200 in Russia,[27] the Advanced Lead-Cooled Fast Reactor European Demonstrator (ALFRED),[28] and the ELSY[29] in Italy.

While the previous study focused on ASTRID SFR system, the current study focuses on the ELSY LFR system, which provides accessible information regarding geometry, material balance, and operational conditions.[30] The core layout of ELSY is shown in Figure 2, and the main characteristics are summarized in Table 2. The active core height of ELSY (120 cm) is very close to that of the ASTRID (about 110 cm), and the two systems share the same thermal power level (1500 MWth). However, the ASTRID core is much more compact due to its axial heterogeneity, which requires higher PuO_2 content in its MOX fuel. Furthermore, the ELSY core diameter is larger than that of the ASTRID core.

Considering SCA in ELSY, two configurations are considered as extremes. The first configuration consists of a full blockage of a coolant channel and meltdown of

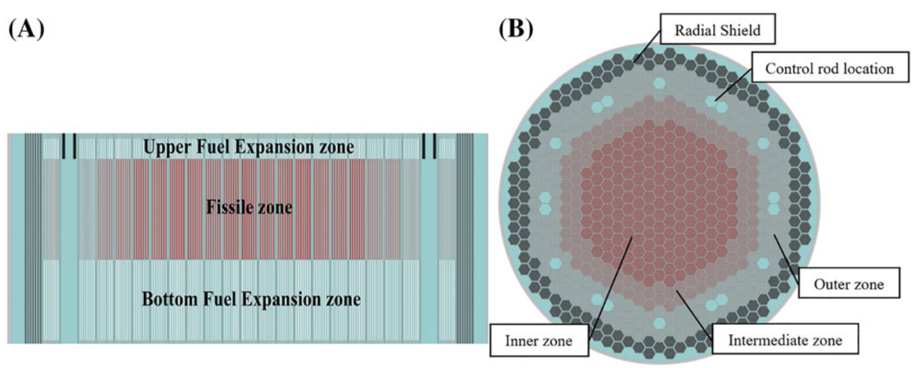

FIGURE 2 ELSY core layout: (A) axial cut and (B) radial cut [Colour figure can be viewed at wileyonlinelibrary.com]

TABLE 2 Design parameters for the ELSY core[29-31]

Core design parameter	ELSY
Nominal thermal power, MWth	1500
Primary coolant	Lead
Core dimensions	
• Lower fuel expansion zone, cm	96
• Fissile zone, cm	120
• Upper fuel expansion zone, cm	24
• Core radius, cm	290
• Assembly pitch, cm	21.6
Fissile zone PuO_2 enrichment (inner/intermediate/outer), %	14.5/15.5/18.5
Effective delayed neutron fraction (β_{eff}), pcm	355
Reactivity worth of 100% void, $	−12

the fuel, followed by stratification of materials, ie, fuel on the bottom and structural materials on top, with a void above. The second configuration is similar to the first one with a single difference, ie, the presence of lead on top of the melted zone. The different degraded configurations are shown in Figure 3.

3 | RESULTS AND DISCUSSIONS

This section deals with the design of a representative experimental program in a ZPR related to neutronic effects during severe core accidents in Gen-IV reactors. First, uncertainty propagation of the ELSY reactor is presented, followed by a short summary of the ASTRID uncertainty analysis. Second, the methodology previously developed for the optimal design of the experimental program on a single fuel assembly level[17] is executed with respect to a single ELSY fuel assembly degraded states (Figure 3). Finally, based on the lessons learned from the study on a single ELSY fuel assembly, the representativity of a single degraded ASTRID fuel assembly is revisited.

3.1 | Uncertainty propagation in the ELSY design

The uncertainty propagation enables a better understanding of the neutronic characteristics of the reactor under investigation. For the ELSY design, the uncertainty propagation is performed using the ENDF/B-VII.1 nuclear data evaluation, in 175 energy groups. The utilization of additional nuclear data library with a fine energy mesh (175 groups for ENDF vs 33 groups for JEFF-3.1.1) provides further verification of the models' flexibility in the design of the experimental program.

The results of the uncertainty propagation on the multiplication factor are given in Table 3 and Figure 4. The results indicate that there are *six* major isotopes that contribute to the total propagated uncertainties, ie, ^{56}Fe, ^{206,207}Pb, ^{238}U, and ^{239,240}Pu. The propagation of uncertainties, performed with the ENDF covariance data, follows the same trend obtained with the JEFF covariance data evaluation,[32,33] similarly to previous analysis of experimental programs related to SCA studies (the SNEAK-12A/B experimental program[34,35]). The uncertainty related to ^{238}U and ^{239}Pu remains high in the two different evaluations. Furthermore, the total propagated uncertainty related to ND remains at a magnitude of ~1000 pcm, which is similar to the uncertainty estimation performed for the ASTRID core (Section 3.2).

The uncertainty propagation analysis (Table 3) reveals interesting behavior regarding individual isotopes' contribution to the propagated uncertainties. The isotopic composition used in ELSY is of natural lead, where the isotopic breakdown is.

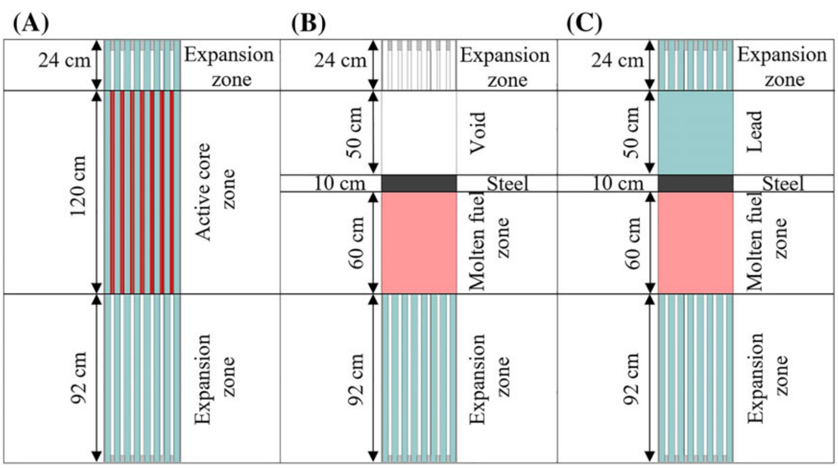

FIGURE 3 Degraded configuration considered in ELSY SCA studies. A, Reference intact ELSY fuel assembly. B, Molten ELSY fuel zone with a void on top. C, Reflooded molten pool [Colour figure can be viewed at wileyonlinelibrary.com]

TABLE 3 Breakdown of total propagated uncertainties for ELSY core [pcm]

Isotope	Capture	Elastic Scattering	Fission	Inelastic Scattering	N,xN	Total
^{56}Fe	20.2	305.2	0.0	83.6	0.0	317.1
^{204}Pb	31.5	1.6	0.0	8.1	0.1	32.6
^{206}Pb	21.0	19.4	0.0	110.6	1.1	114.2
^{207}Pb	43.3	23.0	0.0	135.3	1.9	143.9
^{208}Pb	40.8	24.8	0.0	29.0	3.1	55.9
^{235}U	47.6	0.1	11.0	1.8	0.0	48.9
^{238}U	355.8	9.2	32.1	766.0	4.1	845.3
^{239}Pu	287.5	1.0	207.3	86.5	0.3	364.9
^{240}Pu	138.7	0.6	18.5	35.4	0.1	144.3
^{241}Pu	0.0	0.6	54.5	24.1	0.3	59.6
Total	486.0	307.8	217.8	796.6	5.6	1006.4

Isotope	^{204}Pb	^{206}Pb	^{207}Pb	^{208}Pb
Abundance	1.4%	24.1%	22.1%	52.4%

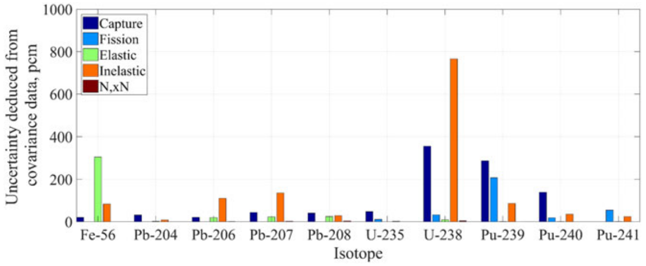

FIGURE 4 Propagated uncertainties, associated with the criticality level of the system (k_{eff}), for the ELSY core with ENDF/B-VII.1 covariance data[20] [Colour figure can be viewed at wileyonlinelibrary.com]

The uncertainties associated with the inelastic scattering show that although ^{208}Pb is the most abundant isotope, it does not exhibit the highest propagated uncertainty. Moreover, its propagated uncertainty is not much higher than the uncertainty related to ^{204}Pb. Furthermore, the propagated uncertainty for inelastic scattering is much lower for ^{208}Pb than for ^{206,207}Pb. This behavior is associated with the inelastic scattering cross section of the lead isotopes, as shown in Figure 5, which is a threshold reaction. The above behavior results from the difference in the energy thresholds for the different isotopes, with the ^{204}Pb threshold being the highest with respect to the other isotopes. Moreover, the uncertainties associated with inelastic scattering cross section of ^{208}Pb are substantially lower with respect to the other isotopes.

Thus, the impact of the different lead isotopes on the propagated uncertainties of the ELSY design exhibit

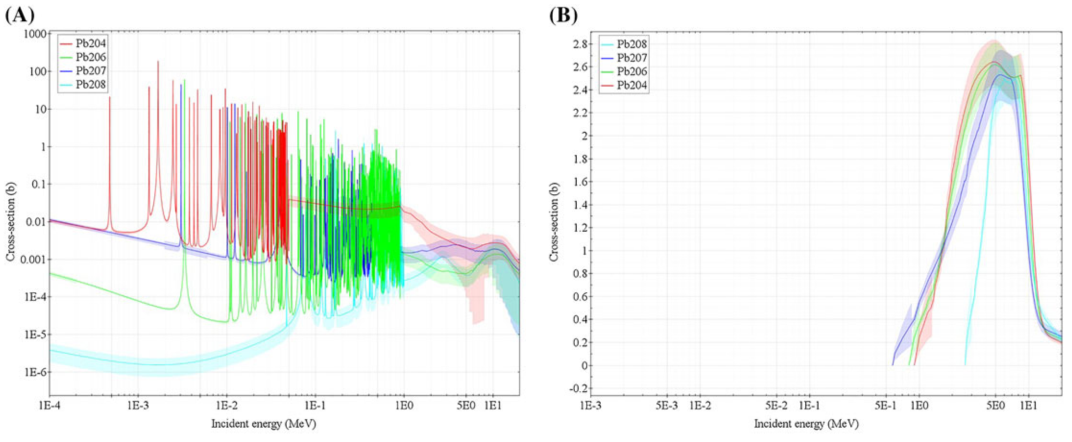

FIGURE 5 Inelastic scattering cross section for the different lead isotopes from ENDF/B-VII.1 evaluation [Colour figure can be viewed at wileyonlinelibrary.com]

complex behavior, which depends not only on the isotopic abundance but on the nuclear data as well.

3.2 | Uncertainty propagation in the ASTRID design

The main contributors to the total uncertainty of the ASTRID core are the heavy isotopes ^{238}U and ^{239,240}Pu (Figure 6). The total propagated uncertainty in the ASTRID core reaches 1400 pcm, which is slightly higher than that of the ELSY core. The main difference (with respect to the ELSY core) is observed in the capture of ^{238}U and fission of ^{239,240}Pu, attributed to their reduced uncertainties in ENDF in comparison with COMAC-V01 (Appendix A).

The differences in uncertainties on ^{56}Fe are much lower for the ASTRID than for ELSY. This is mainly related to the different covariance data used for ELSY (Figure 4, ENDF) and ASTRID (Figure 6, COMAC-V01). Moreover, the spectrum is slightly different between the two designs, so any slowing down variations in inelastic scattering of iron will be strongly amplified (threshold reaction).

Thus, the isotopes considered for representativity in the two systems are similar, ie, ^{238}U, ^{239,240,241}Pu, and ^{56}Fe. Therefore, the only difference between the two systems in terms of representativity calculations is the coolant type, ie, ^{23}Na for ASTRID and ^{204,206,207,208}Pb for ELSY.

At this point of the study, it is reasonable to assume that it is possible to design high representativity experimental ZEPHYR configuration for high-temperature reactivity variations in an ELSY fuel assembly. This argument is supported by the great similarity between the propagated uncertainties in the two Gen-IV systems, the ELSY and the ASTRID, and by the fact that high representativity was already obtained for high-temperature reactivity variations in an ASTRID fuel assembly. The highly representative experimental ZEPHYR configurations would be achieved by identifying the relationship between temperature effects in ELSY and density effects in ZEPHYR.

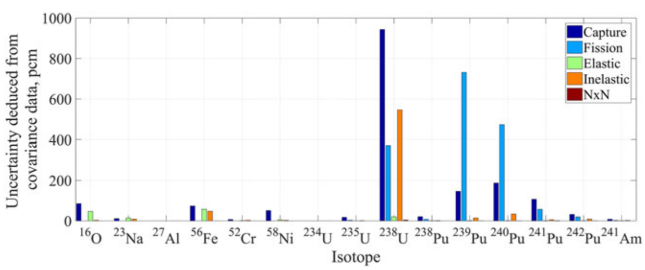

FIGURE 6 Propagated uncertainties, associated with the criticality level of the system (k_{eff}), for the ASTRID CFV-V0 core with COMAC-V01[7] [Colour figure can be viewed at wileyonlinelibrary.com]

3.3 | Representativity of a single degraded ELSY fuel assembly

The results presented in this section are obtained utilizing the same optimization methodology that was presented for the ASTRID assembly degradation in a previous study.[7] The study is concentrated on the temperature variation from 900°C at the nominal state to 3000°C at the degraded configuration of the ELSY fuel assembly. The optimization methodology utilizes particle swarm stochastic optimization (PSO) algorithm,[36] for the maximization of the representativity factor through the search for the "perfect fuel" that will ensure the highest r_{RE} value.

The term perfect fuel refers to a hypothetical representative ZEPHYR fuel assembly with such plutonium oxide content that provides the highest representativity of the power system. The optimal plutonium content is a degree of freedom of the optimization process and theoretically can assume any value between 0% and 100%. This is in contrast to, eg, the "MASURCA fuel," which is an existing fuel repository of the MASURCA fast critical assembly and is comprised of fuel element of different geometries and different plutonium contents.

The examined configurations that would be loaded into the ZEPHYR facility are shown in Figure 7. The reference fuel assembly for the representativity studies (Figure 7A) is a square type lattice that is loaded with eight lead rodlets, two natural UO_2 pins, and six MOX pins. This type of fuel assembly was found to be the most representative of the ELSY undegraded fuel assembly and is thus loaded into the ZEPHYR core. Consequently, the multiplication factor representativity of a single fuel ELSY assembly reaches a value of 0.96. The two degraded configurations that are considered are a meltdown of the MOX fuel and the formation of a molten region with material stratification, without and with lead reflooding of the voided zone above the melted fuel (Figure 7B and 7C, respectively).

In the previous study of a single ASTRID fuel assembly,[7] a variety of temperatures were considered for research purposes. In this study, only realistic conditions are examined, ie, temperatures of 900°C for normal core operation conditions and of 3000°C for degraded configurations. The results of the PSO calculations are given in Table 4 and Figure 8. The results show that in the case of the LFR core, the representativity exhibits a distinct behavior as a function of plutonium content. Unlike in the SFR single degraded zone simulations, where only a

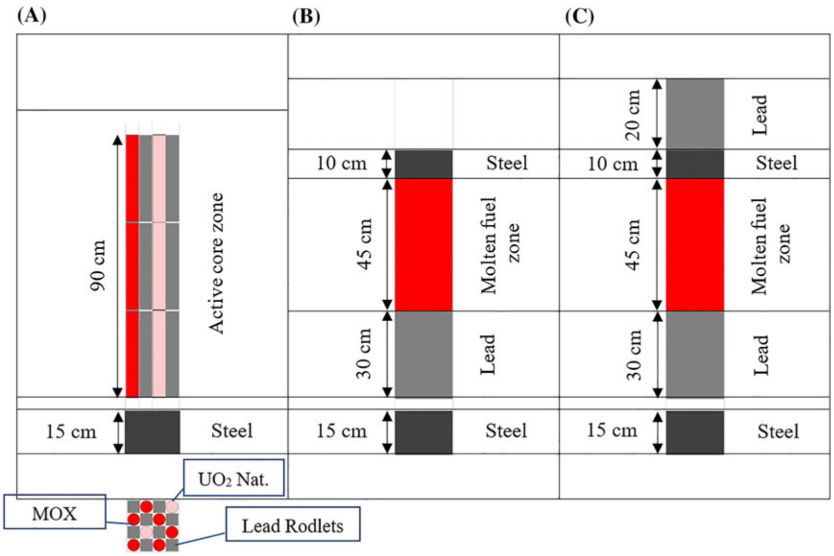

FIGURE 7 Fuel assembly configuration for representativity studies of ELSY SCA to be loaded into ZEPHYR. A, Reference. B, Degraded configuration 1: void above melt. C, Degraded configuration 2: lead above melt [Colour figure can be viewed at wileyonlinelibrary.com]

TABLE 4 Representativity of reactivity variations for the different degraded ELSY configuration and the optimal plutonium content in the ZEPHYR fuel

Core	Degraded Configuration	PuO_2 Content in MOX	r_{RE}
ELSY (ENDF/B-VII.1)	Ref. to deg. config. 1	19.8%	0.96
	Ref. to deg. config. 2	18.8%	0.96

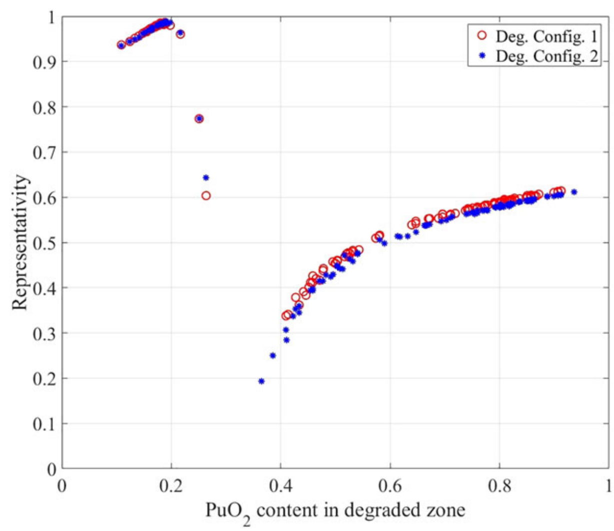

FIGURE 8 PSO results for the representativity of a single degraded ELSY fuel assembly [Colour figure can be viewed at wileyonlinelibrary.com]

single point gives representativity value above 0.85, in the LFR case, a wide range of plutonium content exist (below 20%) with representativity values above the required value of 0.85. Around 25% PuO_2 content, the representativity drops sharply, and as the content of the PuO_2 is further increased, the representativity monotonically increases towards an asymptotic value of around $r_{RE} = 0.6$.

The comparison of the sensitivity profiles of the reactivity variations (Figure 9) in the ZEPHYR vs the ELSY systems shows that the sensitivity profiles are very similar, especially, for the capture in ^{238}U and fission of ^{239}Pu, which are the dominant reactions in both systems.

3.4 | Revisiting the representativity of a single degraded ASTRID fuel assembly

In light of the excellent results for the single ELSY fuel assembly degradation representation, a revisit of the results obtained for the single ASTRID fuel assembly degradation is performed, mainly in order to estimate the impact of different nuclear data library and finer structure of energy groups (COMAC—33 groups, ENDF—175 groups) on the representativity process.

Previous results, obtained using JEFF-3.1.1 and COMAC,[7] show that the target representativity factor of 0.85 can be obtained just for a very narrow range of PuO_2 content values. However, a change in both the nuclear-evaluated data set and the associated covariance matrix can substantially alter the results. For example, changing only the covariance matrix from COMAC to updated covariance matrix (UCOM)[37] increases the required PuO_2 content without changing the maximal representativity factor of 0.85.[7] The increase in PuO_2 content, in this case, is due to the increased importance of ^{240}Pu in the representativity process. Utilizing the ENDF and its associated covariance data with finer energy mesh (175g vs 33g) leads to increase in representativity (0.91), probably because less information is lost during

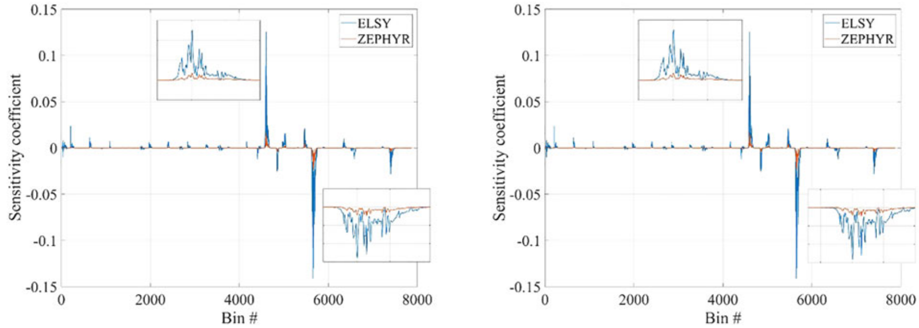

FIGURE 9 Sensitivity profiles of the reactivity variations in the ZEPHYR and ELSY. A, Ref. vs deg. config. 1. B, Ref. vs. deg. config. 2. The insets show "zoom-in" on the large peaks [Colour figure can be viewed at wileyonlinelibrary.com]

downscaling (coarse meshing) of the covariance matrix. Both revisited ASTRID and ZEPHYR configurations are shown in Figure 10, and the results of the representativity analysis are summarized in Table 5.

In the previous analysis, it was demonstrated that the representativity results are strongly linked to the uncertainty level.[7] For example, when the uncertainties were reduced for key isotopes and reactions (ie, ^{238}U and ^{239}Pu), the representativity level dropped. This is due to the increase in the relative importance of other isotopes in the representativity process, which may behave differently in the experimental system.

In this study, three main reactions govern the representativity process in all examined systems, ie, capture and inelastic scattering of ^{238}U and fission of ^{239}Pu. The covariance data from COMAC-V01 in 33 groups and from ENDF in 175 groups are shown in Figures A1, A2, and A3 in the Appendix.

Noticeable differences in the uncertainty vectors of all the presented reactions are observed. The uncertainties associated with ENDF covariance data are notably lower with respect to the COMAC-V01 data. The impact of the uncertainty reduction of the representativity process was previously examined by reducing the uncertainties in COMAC and the generation of UCOM.[37] This change led to the increase in the required amount of PuO_2 in the degraded MOX zone in order to achieve the required level of representativity (Table 5). The change in the PuO_2 content stems from the different plutonium vectors associated with the ASTRID and with the ZEPHYR, where

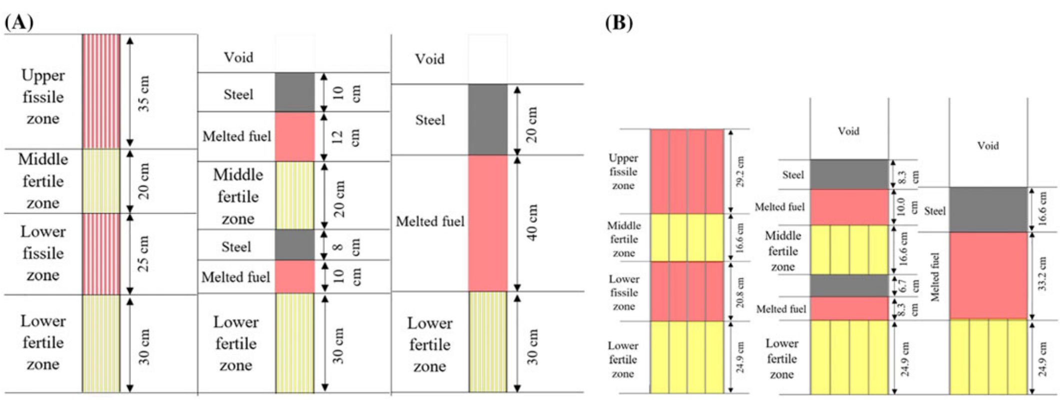

FIGURE 10 Revisited degraded configurations of a single ASTRID fuel assembly,[7] from voided fuel assembly to a single molten zone (note: the figures are not on the same scale). A, ASTRID configurations. B, ZEPHYR configurations [Colour figure can be viewed at wileyonlinelibrary.com]

TABLE 5 Plutonium vectors

System	^{238}Pu	^{239}Pu	^{240}Pu	^{241}Pu	^{242}Pu	^{241}Am
ASTRID[39, 40]	3%	55%	26%	7%	7.5%	1.5%
ELSY[29,30]	2.3%	57%	27%	6.1%	7.6%	-
ZEPHYR	0.8%	70%	18%	8%	2%	0.2%

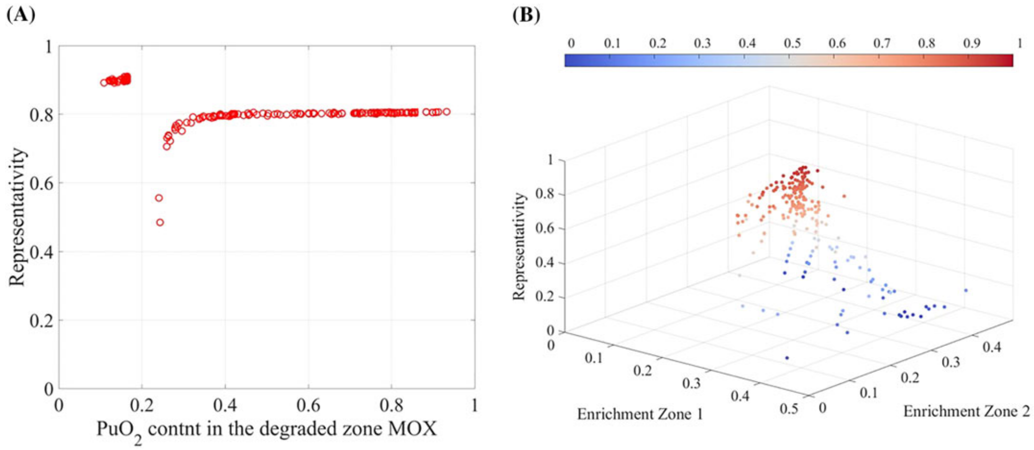

FIGURE 11 Representativity results of degraded situations using ENDF covariance. A, Single zone. B, Two zones [Colour figure can be viewed at wileyonlinelibrary.com]

TABLE 6 Optimized plutonium content of the ZEPHYR fuel using different ND data

Covariance Data Source	Ref. to Single Deg. Zone	r_{RE}	Ref. to Two Deg. Zones Zone 1	Zone 2	r_{RE}
COMAC-V01	22.5%	0.85	20%-24%	20%-24%	0.85-0.87
UCOM-V01AB	25.2%	0.85	22.5%-26.5%	22.5%-26.5%	0.85-0.91
ENDF covariance	22%	0.96	25%-30%	15%-20%	0.90-0.94

[a]Reference configuration at 900°C.

[b]Degraded configuration at 1000°C.

[c]COMAC and UCOM given in 33 energy groups and ENDF in a 175 energy groups.

the latter contains much less ^{240}Pu. Hence, the weight of ^{240}Pu in the representativity process is drastically increased due to the reduction in the uncertainties in ^{238}U and ^{239}Pu.

Although JEFF and ENDF are two separate evaluations, the data collapsing to energy groups leads to a change in the shape of the correlation matrix. The correlation between the different energy groups (off-diagonal terms) is smoothed out in the 33g with respect to the 175g. This is despite the fact that the collapse of the covariance matrix to a small number of energy groups conserves the propagated uncertainty.[38] In the case of the representativity process, this energy group collapse may have a profound impact on the value of r_{RE}, as in the current study, since some information is inevitably being lost during the collapsing process.

The impact on the search space shape due to the change in the covariance data is also significant, as shown in Figure 11. The overall behavior is similar to the previous findings, with three zones, ie, the relatively low representativity values at high PuO_2 contents, a "death valley" cutoff, and the high representativity region. However, when using the previous 33g covariance data, the high representativity region is represented by a single point, whereas in the current case (of 175g), this region is much wider. Nevertheless, the two different libraries achieve the required representativity value around the same PuO_2 content, ie, around 22%. The three approaches are summarized in Table 6.

4 | SUMMARY AND CONCLUSIONS

This paper presents the continuous effort put in the design of a novel experimental program related to Gen-IV SCA studies in the future ZEPHYR versatile critical facility to be constructed around 2028 at Cadarache, France. This novel experimental program belongs to a new class of representative experiments, where zero-power critical facilities (eg, ZEPHYR) are utilized for studying severe core accidents and reactivity effects in power reactors and in high temperatures. This paper summarizes the additional capabilities developed for this experimental program.

This study is a significant augmentation of the previously designed innovative heuristic approach, which is based on coupling Monte Carlo sensitivity calculation with advanced stochastic optimization method. In this study, the modeling capabilities in the ZEPHYR are extended beyond SFR to include also Gen-IV LFR designs.

The capability extension to include Gen-IV lead-cooled fast reactors is carried out using the design of the ELSY serving as a reference system. The study addresses the challenges related to the design of a representative experiment for a single degraded ELSY fuel assembly. Due to the lack of covariance data related to lead in COMAC-V01, the ENDF covariance data were utilized in 175 energy groups.

Considering SCA in ELSY, two configurations are considered as extremes (eg, Figures 3 and 7). The two degraded configurations represent a meltdown of the MOX fuel and the formation of a molten region with material stratification, without and with lead reflooding of the voided zone above the melted fuel (eg, Figure 7B and 7C, respectively). The design optimization process reveals that it is possible to identify highly representative configurations, to be loaded into the ZEPHYR core, of the reactivity variation related to ELSY, as shown in Figure 8 and detailed in Table 4.

The sensitivity of the representativity process to the energy group structure of the covariance matrices is examined using both JEFF and ENDF evaluations. For this purpose, the representativity of a single degraded ASTRID fuel assembly is revisited. This energy group collapse is shown to induce a profound impact on the value of the representativity factor since some information is bound to vanish during the collapsing process. For example, the correlation between the different energy groups is smoothed out in the JEFF 33 g with respect to the ENDF 175 g (eg, Figures A1–A3). It is also shown that not only the maximal representativity value is strongly affected by the energy group structure of the covariance data. The shape of the search space itself, as sampled by the PSO process, is also significantly affected (Figure 11). Finally, it is demonstrated that the finer group structure of the covariance data eventually results in better representativity values and more robust design optimization process (Table 6).

By extending the proposed representative experimental program to two Gen-IV systems, the flexibility of the ZEPHYR facility is enhanced such that it can accommodate almost any other Gen-IV system characterized by different fuels and coolants.

The main novelty of the proposed methodology remains the representativity of high-temperature effects, which characterize power systems, and their expression by variations in the content of the plutonium oxide in the fuel of the ZPR. In this study, this novel methodology is further qualified by applying it to study a single fuel assembly SCA in the ELSY design, and successfully obtaining high representativity values. This study is a necessary preliminary step towards further qualification of the methodology on a full core SCA for both the SFR and LFR cores in the ZEPHYR facility.

ACKNOWLEDGEMENTS

The research was partially funded by the Israeli Ministry of Energy, contract number 215-11-020.

ORCID

Marat Margulis https://orcid.org/0000-0002-7188-3301
Patrick Blaise https://orcid.org/0000-0003-4609-5351
Erez Gilad https://orcid.org/0000-0002-2130-9301

REFERENCES

1. International Atomic Energy Agency. *The Fukushima Daiichi accident*. Vienna; 2015 GC(59)/14.
2. Sehgal BR (Ed). *Nuclear Safety in Light Water Reacctors*. 1st ed. Amsterdam: Academic Press; 2012.
3. Van Dorsseleare JP, Albiol T, Micaelli JC. Research on severe accidents in nuclear power plants. In: Tsvetkov P, ed. *Nuclear Power - Operation, Safety and Environment*. Rijeka: INTECH; 2011.
4. Bathe HA, Tait JH. *An Estimate of the Order of Magnitude of Vigorous Interaction Expected Should the Core of a Fast Reactor Collapse*. Risley: U.K.a.AReactor Group; 1956.
5. Bohl WR. Some Recriticality Studies with SIMMER-II. Paper presented at: international meeting on fast reactor safety technology, 1979; Seattle, WA, USA.
6. GIF. *A Technology Roadmap for Generation IV Nuclear Energy Systems*. Paris: GIF; 2014.
7. Margulis M, Blaise P, Gilad E. Modeling representative gen-IV molten fuel reactivity effects in the ZEPHYR fast/thermal coupled ZPRs. Part I—assembly level. *Int J Energ Res*. April 2018;42(5):1950-1972.
8. Maschek W, Munz CD, Meyer L. Investigations of sloshing fluid motions in pools related to recriticalities in liquid-metal fast breeder reactor core meltdown accidents. *Nucl Tech Apri*. 1992;98(1):27-43.
9. Dos Santos N, Blaise P, Santamarina A. A global approach of the representativity concept application on a high-conversion submoderated MOX lattice case. Paper presented at: M&C-2013, 2013; Sun Valley, ID, USA.
10. Lebrat JF, Tommasi J. The use of representativity theory in the depletion calculations of SFR blankets. *Ann Nucl Energ*. 2017;101:429-433.
11. Bertrand F, Marie N, Prulhiere G, Lecerf J, Seiler JM. Comparison of the behaviour of two core designs for ASTRID in case of severe accidents. *Nucl Eng Des*. 2016;297:327-342.

12. Asahi Shimbun. Scaling back of French reactor a blow for nuke fuel reprocessing. The Asahi Shimbun May 31, 2018. Available at: http://www.asahi.com/ajw/articles/AJ201805310040.html. Accessed May 31, 2018.
13. Blaise P, Boussard F, Leconte P, et al. Experimental R&D innovation for Gen-II,III & IV neutronics studies in ZPRs: a path to the future ZEPHYR facility in Cadarache. Paper presented at: IGORR-2016, 2016; Berlin, Germany.
14. Alemberti A, Carlsoon J, Malambu E, et al. European lead fast reactor ELSY. *Nucl Eng Des*. 2011;241(9):3470-3480.
15. Orlov VV. Problem of fast reactor physics related to breeding. *At Energy Rev*. 1980;January;989-1077.
16. WNN. Molten salt reactor experiment begins at Petten. World Nuclear News. September 06, 2017. Available at: http://www.world-nuclear-news.org/NN-Molten-salt-reactor-experiment-begins-at-Petten-0609174.html.
17. Rahnema F, Diamond D, Serghiuta D, Burke P. Phenomena, gaps, and issues for neutronics modeling and simulation of FHRs. *Ann Nucl Energ*. 2019;123:172-179.
18. Ronen Y. *Uncertainty analysis*. CRC Press; 1988.
19. Chadwick MB, Herman M, Obložinský P, et al. ENDF/B-VII.1: nuclear data for science and technology: cross sections, covarinaces, fission product yields and decay data. *Nucl Data*. 2011;112(12):2887-2996.
20. Soppera N, Bossant M, Dupont E. JANIS 4: an Iproved version of the NEA Java-based nuclear data information system. *Nucl Data*. 2014;120:294-296.
21. Aufiero M, Bidaud AV, Hursin M, et al. A collison history-based approach to sensitivity/pertubation calculations in the continues energy Monte Carlo code serpent. *Ann Nucl Energ*. 2015;85:245-258.
22. Dos Santos N. *Optimisation de l'approche de représentativité et de transposition pour la conception neutronique de programmes expérimentaux dans les maquettes critiques*. Grenoble: Universite de Grenoble; 2013.
23. Chenaud MS, Devictor N, Mignot G, et al. Status of the ASTRID cccore at the end of the pre-conceptual design phase 1. *J Nucl Eng Tech*. 2013;45(6):721-730.
24. Cacuci DG (Ed). *Handbook of Nuclear Engineering*. 1 New York: Springer; 2010.
25. Piro IL (Ed). *Handbook of Generation IV Nuclear Reactors*. Cambridge: Woodhead Publishing; 2016.
26. Aït Abderrahim H. Multi-purpose hYbrid research reactor for high-tech applications a multipurpose fast spectrum research reactor. *Int J Energ Res*. December 2012;36(15):1331-1337.
27. Dragunov YG, Lemekhov VV, Moiseev AV, Smirnov VS. Lead-cooled fast-neutron reactor (BREST). Paper presented at: 48th Meeting IAEA TWG FR, 2015; Obninsk.
28. Ponciroli R, Cammi A, Lorenzi S, Luzzi L. A preliminary approach to the ALFRED reactor control strategy. *Progr Nucl Energ*. May 2014;73:113-128.
29. Alemberti A, Carlsoon J, Malambu E, et al. European lead fast reactor—ELSY. *Nucl Eng Des*. September 2011;241(9):3470-3480.
30. Ghasabyan LK. Use of Serpent Monte-Carlo code for development of 3D full-core models of Gen-IV fast-spectrum reactors and preparation of group constants for transient analyses with PARCS/TRACE coupled system. Stockholm: KTH Engineering Sciences; 2013.
31. NEA. *Homogeneous versus Heterogeneous Recycling of Transuranics on Fast Nuclear Reactors*. Paris: OECD/NEA; 2012.
32. Margulis M, Blaise P, Mellier F, Gilad E. The path for innovative severe accident neutronics studies in ZPRs. Part I.2—impact of nuclear data uncertainties on reactivity changes of SNEAK-12A core. *Progr Nucl Energ*. 2017;96:97-117.
33. Margulis M, Blaise P, Millier F, Gilad E. The path for innovative severe accident neutronics studies in ZPRs. Part II.2—impact of nuclear data uncertainties on reactivity changes of SNEAK-12B core. *Progr Nucl Energ*. May 2018;105:124-138.
34. Margulis M, Blaise P, Gabrielli F, Gruel A, Mellier F, Gilad E. The path for innovative severe accident neutronics studies in ZPRs. Part I.1—analysis of SNEAK-12A experiments for core disruption in LMFBRs. *Progr Nucl Energ*. 2017;94:106-125.
35. Margulis M, Blaise P, Gabrielli F, Gruel A, Mellier F, Gilad E. The path for innovative severe accident neutronics studies in ZPRs - Analysis of SNEAK-12B experiments for core disruption in LMFBRs. *Ann Nucl Energ*. 2019;124:119-131.
36. Kennedy J, Eberhart RC. Swarm intelligence: Morgan Kaufmann; 2001.
37. Margulis M, Blaise P, Rimpault G, Gilad E. Interpretation of the SNEAK-12A/B experimental programs on severe core accidents in LMFBRs Some feedback on nuclear data re-assimilation for the prediction of reactivity changes. Paper presented at: ICAPP-2017, 2017; Fukui/Kyoto, Japan.
38. Hiruta H, Palmiotti G, Salvatores M, Arcilla R Jr, Obložinskýc P, McNight RD. Few group collapsing of covariance matrix data based on a conservation principle. *Nucl Data*. December 2008;109(12):2801-2806.

How to cite this article: Margulis M, Blaise P, Gilad E. Modeling representative Gen-IV molten fuel reactivity effects in the ZEPHYR ZPR - LFR analysis. *Int J Energy Res*. 2019;43:829–843. https://doi.org/10.1002/er.4313

APPENDIX A

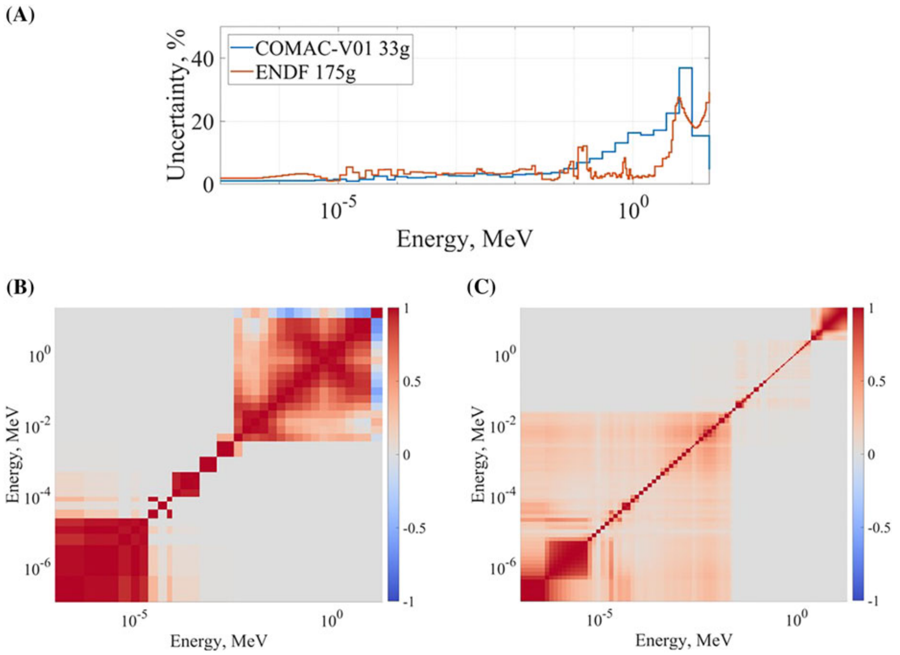

FIGURE A1 Covariance data for capture of ^{238}U. A, Uncertainty vector comparison. B, COMAC-V01 correlation matrix. C, ENDF correlation matrix [Colour figure can be viewed at wileyonlinelibrary.com]

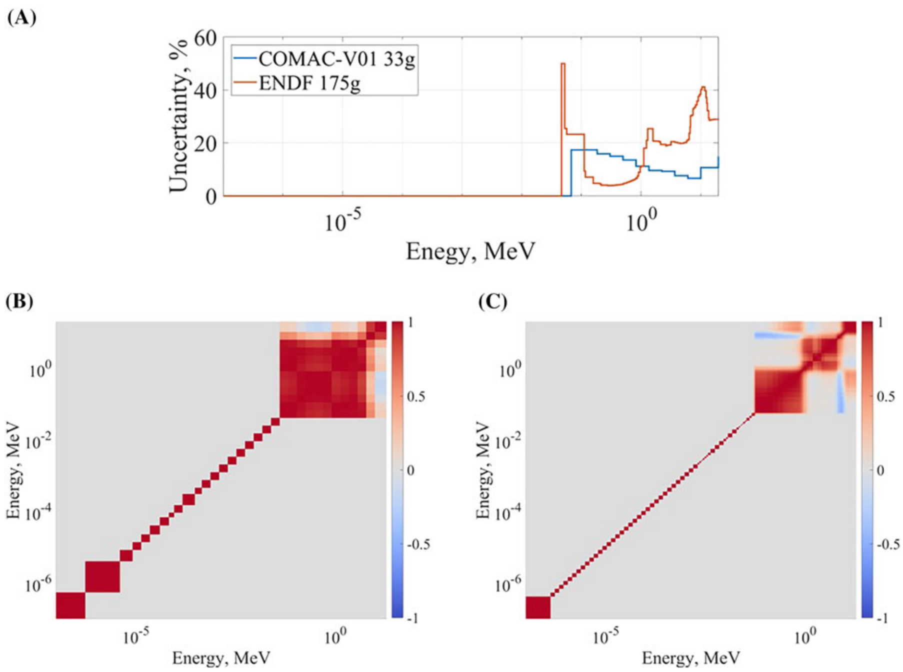

FIGURE A2 Covariance data for inelastic scattering of ^{238}U. A, Uncertainty vector comparison. B, COMAC-V01 correlation matrix. C, ENDF correlation matrix [Colour figure can be viewed at wileyonlinelibrary.com]

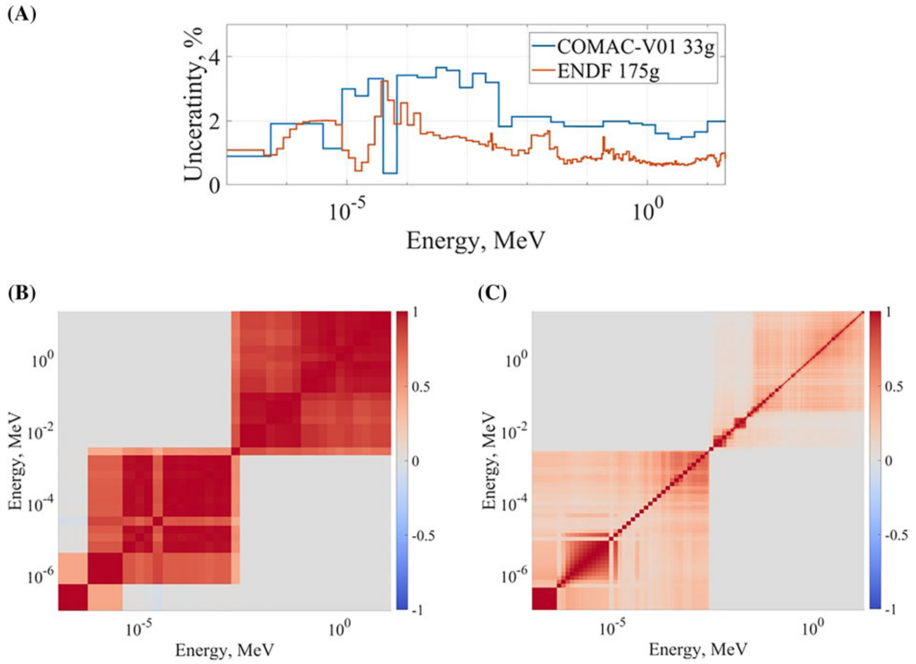

FIGURE A3 Covariance data for fission of ^{239}Pu. A, Uncertainty vector comparison. B, COMAC-V01 correlation matrix. C, ENDF correlation matrix [Colour figure can be viewed at wileyonlinelibrary.com]